Observation of universal "ageing" dynamics in antibiotic persistence

Yoav Kaplan, Shaked Reich, Elyaqim Oster, Shani Maoz, Irit Levin-Reisman, Irine Ronin, Orit Gefen, Oded Agam and Nathalie Q. Balaban

Racah Institute of Physics, Edmond J. Safra Campus, The Hebrew University of Jerusalem, Jerusalem 9190401, Israel.

Stress response in cells is understood as an organized response that allows cells to adapt to changes in external conditions by activating specific pathways. Here we investigate the dynamics of single cells when perturbed by an acute stress that is too strong for a regulated response but not lethal. We show that when the growth of bacteria is arrested by transient exposure to strong inhibitors, the statistics of their regrowth dynamics can be predicted by a model for the cellular network that ignores most of the details of the underlying molecular interactions. By measuring the regrowth dynamics after stress exposure on thousands of cells, we show that the model can predict the outcome of antibiotic persistence measurements. Further experiments under different stress conditions support the predictions of the model. Our results may account for the ubiquitous antibiotic persistence phenotype, as well as for the difficulty in attempts to link it to specific genes. More generally, our approach suggests that two different cellular states can be observed under stress: a regulated state, which prepares cells for fast recovery, and a disrupted cellular state due to acute stress with slow and heterogeneous recovery dynamics. The latter may be described by general properties of large random networks rather than by specific pathway activation. Better understanding of the disrupted state could shed new light on the survival and evolution of cells under stress.

Stress responses at the level of a single cell have been studied in many biological systems[1,2]. For example, when nutrients become scarce, cells can adapt by upregulating intracellular production, increasing import or switching to a different metabolism that prepares cells for survival, and regrowth when nutrients become available[3]. Many stress response pathways have been mapped, leading to the understanding of the mechanisms used by cells to cope with changing conditions[4]. However, when subjected to acute stress, which is too strong for the stress response to kick in, the behavior of cells is much less understood. In particular, even under mild stress, some sub-populations of cells may be in a disrupted state that prevents them from upregulating a stress response. Evidence for such single cell heterogeneity under stress is found in many different organisms. An example of such

heterogeneity is observed in triggered antibiotic persistence[5-7]. When microorganisms are exposed to starvation, or other stresses, resulting in growth arrest, a small sub-population is frozen in a dormant state which is maintained for a long time even when the cells are transferred back to growth conditions. An example of this extended lag time is shown in Fig. 1. After a period of growth, *E.coli* bacteria reached starvation, arresting their growth. When starvation conditions were replaced with fresh medium (Fig. 1A), bacteria resumed growth stochastically and the lag time for each bacterium was determined using an automated system (ScanLag setup[8]). A typical lag time distribution is shown in Fig. 1B. In contrast to the majority population that was able to resume growth shortly after being switched to fresh nutrients, a tail of long lag bacteria is observed. While this transient dormant state typically bears a fitness cost, it becomes protective if the dormant cells are then exposed to lethal antibiotics which require active growth to kill the bacteria[6,9-11] (Fig. 1A). This better ability of dormant cells to survive is distinct from resistance, which allows bacteria to grow in the presence of antibiotics[7]. In Fig. 1C we show that the antibiotic persistence level, i.e. the fraction of surviving bacteria after an antibiotic treatment, correlates with the tail of the lag time distribution. Because the antibiotic is not effective for killing the non-growing bacteria (still in the lag phase), the bacteria that have a lag time longer than the antibiotic treatment are protected, also termed "persistence-by-lag"[12,13]. This result is in agreement with previous findings[8,14-16] and was reproduced using strains and conditions that span different triggered persistence levels (Fig. 1C). We conclude that understanding what shapes the stochastic exit from dormancy, i.e. the lag time distribution, enables predicting the triggered persistence level, as studied below.

Despite 20 years of research into the pathways regulating antibiotic persistence[17] and leading to the long lag bacteria, no clear unified molecular understanding of this clinically relevant phenotype[18] has emerged. In this work, we show that the extended lag is the result of bacteria unable to overcome the stressful conditions imposed by starvation and entering a disrupted state. More generally, we propose a theoretical and experimental framework for the analysis of dynamics of cells exposed to acute stress which is beyond their adaptive potential, but not lethal, leading to a disrupted state. We focus on the quantitative measurements of the recovery of single cells from the disrupted state and show that they can be described by the general features of a model that ignores most of the details of

specific cellular pathways. The universal behavior predicted by the model was able to predict the antibiotic persistence level as well as the quantitative dynamics of recovery from different stresses.

Memory effect following acute stress

To determine quantitatively how the lag time distribution depends on starvation duration under acute stress conditions, we added serine hydroxamate (SHX) to exponentially growing cultures of *E.coli*. SHX induces the starvation for the amino acid serine which triggers the stringent response and results in a growth arrest[19] (Fig. 2A). In order to impose an acute stress that the bacteria cannot overcome and be further away from a regulated stress response, we used a relaxed mutant of the stringent response. Observations at the single cell level in microfluidic devices show that exposure to SHX results in the growth arrest of the bacteria and rule out that the growth arrest observed at the level of the population is a balance of death and growth (Fig. 2D,E).

We monitored the dynamics of the recovery after the growth arrest imposed by SHX for a duration T_w, by measuring the distribution of lag times once the SHX is removed. In agreement with previous results under other stress conditions[8,14,15], we found that the longer the duration of SHX exposure, the longer the tail of the distribution that dominates the antibiotic persistence level (Fig. 2B,C), with bacteria lagging for more than day . This suggested that the bacteria keep a memory of the total duration of SHX exposure. This memory is not due to stable genetic changes because repeating the same experiment for a culture started from a late appearing colony again depended on the starvation time[8] (Fig. S1C,D). In agreement with recent results, we observed that the distributions display a long tail, which is also reflected in the tail of the killing curve under antibiotic treatments[20]. Whereas an exponential decay is the expected behavior of a stochastic process with one characteristic time and is often observed in the initial killing of microorganisms by antibiotics, the tail of persisters in wild-type *E.coli* cannot be fitted with a single exponential decay[6,20]. One explanation for the appearance of a long tail after SHX exposure may be because the short lag bacteria are killed by the SHX itself, which would enrich for the long lag bacteria. We ruled this factor out by showing that the viability under SHX

stayed nearly constant (Fig. S1A) and by direct observation of *E.coli* bacteria before, during and after exposure to SHX in a microfluidic device[21] (Fig. 2D,E). Delays due to the SHX diffusion were ruled out (Supplementary information). We conclude that the lag time distribution following exposure to SHX reflects the changes that occurred in each single cell, increasing the probability for extremely long recovery times that keep a memory of the starvation duration. In order to further understand this phenomenon, we first search for a theoretical model with similar features.

"Ageing" as a universal property of random highly connected networks

The memory of the duration of a perturbation observed above (here SHX exposure for duration T_w), as well as the non-exponential relaxation, has an equivalent in many physical systems that display "ageing"[22], ranging from amorphous polymers[23], stretched DNA[24], crumpling[25,26], colloidal solutions, spin and coulomb glasses[27]. A physical system exhibits "ageing" if its relaxation after a transient external perturbation of duration T_w depends not only on its macroscopic state at the end of the perturbation but also on the conditions that led to this state[28-30]. For example, Struik[23] showed that the relaxation of amorphous polymers after a deformation depends on how the deformation was done and on its duration. He showed that the behavior was universal i.e. independent of the details of the material, and termed this phenomenon "physical ageing" (thereafter termed ageing), which is distinct from "biological ageing" [31]. Inspired by models for ageing in glassy systems that rely on large random networks[32], we developed a model for the network of intracellular molecular interactions which govern the behavior of each single *E.coli* cell during and after exposure to acute stress. Our goal was to study a generic model, with the minimal assumptions necessary to display the observed ageing dynamics induced by the stress, and without going into the details of the molecular interactions. Similarly to neural networks modelling[33], we considered a network of interacting nodes, while having feedback cycles typical of the genetic and metabolic networks of a cell. The network is built of cycles of various sizes, i.e. the numbers of nodes they contain. Each node represents a compound in the cell's network (proteins, metabolites, etc.) that can be in one of two states representing its current activity[34]. The cycles represent crudely the genetic/metabolic pathways required

for growth, and the distribution of their size was assumed to follow a power law, similarly to the scale-free structure measured on the *E.coli* network[35,36] and protein life-time[37] (see Supplementary Information – Theory). The model, termed the "Randomly Connected Cycles Network" (RCCN), is schematically drawn in Fig. 3A and Box1. Here the up/down green arrows represent nodes in either the ON or OFF state. Exposure to SHX translates in the model as a force applied for duration T_w , tending to turn the nodes OFF, and resulting in a macroscopic state of growth arrest. Washing of SHX ends the stress and the fraction of OFF nodes relaxes back (Fig. S2A). Using the RCCN model simulations, we could observe the ageing dynamics of the relaxation (Fig. S2B). The model can be effectively described by an analytical mean field approximation that reproduces the ageing dynamics of the simulations (Fig. S2B- dashed lines) and provides an intuitive framework for understanding the dynamics of recovery after acute stress (see Supplementary Information-Theory). Ageing in the model is due to a cascade of states that need to relax in the correct order for the whole system to go back to its state before the perturbation. This results in frustration, leading to a disrupted state with a broad distribution of time scales of meta-stable states. Within our model, the lag time for recovery of each single cell is determined by the time for the fraction of OFF nodes to go back to its original value before SHX (Box1). The simulated lag time distributions, for various stress durations T_w, are plotted in Fig. 3B, together with the analytical approximation.

Saturation of ageing in experimental data

Both the simulations and the analytical model (Figs. 3B, S2B and Eq. S8) predict several typical features similar to those observed for physical ageing: *(i)* the lag time distribution depends on the stress duration; *(ii)* the lag time distribution contains many timescales and typically exhibits non-exponential decay; *(iii)* the lag time distribution should stop depending on stress duration for long enough stress, and therefore the persister bacteria fraction should not increase further at long stress exposure durations. We note that these predictions are robust to changes in the model's parameters (Fig. S3).

The first prediction is in agreement with the data of Fig. 2B showing the strong dependence of the lag time distribution on SHX exposure times. The second prediction was confirmed

by plotting the higher statistics data on a log-log scale. In agreement with previous results[20], we observe that the experimental lag time distribution cannot be fitted with an exponential decay and better fitted with a power law (Fig S4A and Table S3). In order to test the third prediction, we exposed the culture to longer durations under SHX (Fig. 3C). As predicted by the model, the effect of SHX stress on the lag time distribution of *E.coli* saturates around T_w>1000 minutes (Fig. 3D). This result is surprising from the biological perspective: biological ageing is typically viewed as a continuous decline in the ability of the system to recover, eventually leading to death[38]. Here we show that, in striking similarity with ageing in physical systems, the recovery distribution is not affected by SHX stress duration, once this duration is longer than the longest time scale of the system. The lag time distribution is similar whether the culture has been under SHX for 1300 or 2000 minutes, and without a significant decline in viability[39] (Fig. S1A). Accordingly, and as predicted from the RCCN model, the triggered persister fraction resulting from the transient SHX exposure and measured directly from the survival under antibiotic treatment does not increase further after 1000 minutes of starvation (Fig.3E).

In order to test whether the ageing behavior and its saturation would generalize to other modes of strong perturbation, we subjected wild-type bacteria culture to antibiotic that blocks translation (Chloramphenicol – CAM), as well as to sodium azide, which resulted in growth arrest due to ATP depletion[40] and persistence (Fig. S8). These two stresses act on different pathways, also different from the ones activated by SHX[41,42]. In similarity to the SHX induced growth arrest, we observed ageing in the recovery dynamics from the growth arrest during CAM exposure (Fig. 4H) or sodium azide (Fig.S5).

We conclude that different acute stresses can lead to ageing in the dynamics of the recovery after the stress, revealing a large cell-to-cell variability.

Gradual starvation

The variability and ageing in the recovery of cells from acute stresses was explained above by the dynamics of a random network recovering from a disrupted state. The model is independent of the details of the cellular interaction network. Clearly, such a network cannot account for the regulated behavior of cells which is the result of billions of years of evolution. Therefore, we expected that when cells are exposed to similar but less acute

stress, genetic stress response pathways should prepare cells for recovery[3,4,43,44] and result in a narrow lag time distribution. In Fig. 4, we compared cultures subjected, as above, to abrupt starvation with SHX (Fig. 4A- dotted line), to bacterial cultures reaching gradual starvation, simply by letting the culture deplete the amino-acids (Fig. 4A-solid line), reaching stationary phase. We observed that, in contrast to the ageing behavior under SHX, gradual starvation did not lead to ageing, i.e. the lag time distribution did not change with starvation duration (Fig. 4C). We ruled out that the difference was due to the SHX itself, as its addition to the starved culture had no influence on the lag time distribution under gradual starvation (Fig. S6A). Furthermore, we also exposed exponentially growing culture to a gradual increase in SHX concentration, reaching the same optical density (OD) as abrupt SHX exposure (Fig. 4D). This gradual exposure to stress did not lead to aging (Fig. 4F). As we expected, despite the similar conditions of the abruptly arrested (Fig. 4G) and gradually arrested cultures (Fig. 4F), the lag time distributions are very different. Whereas the gradual starvation leads to little cell-to-cell variability, with a lag time distribution consistent with a fast stochastic exit with a characteristic time of 50 minutes (Fig. S6B), the abrupt SHX starvation results in a broad distribution with time scales longer than a day (Fig. 3D,4G).

Classifying stresses according to their recovery dynamics

The understanding that strong stresses can drive the cell into a disrupted state, with long and widely distributed recovery time-scales, whereas stresses to which cells are adapted result in fast and organized recovery, allows to classify different stresses. As shown above, gradual starvation in minimal medium, as well as gradual exposure to SHX, allows the *E.coli* cells to adapt and reach a growth arrested state from which they emerge back in a uniform and fast time-scale (Fig. 4B,E). Similarly, starvation in saline solution does not lead to ageing (Fig. S9, S10C). However, previous observations of the lag time distributions of *E.coli* K-12 for different durations of starvation at the stationary phase in LB medium suggested that what may seem as a gradual starvation actually leads, in our framework, to a disrupted state and ageing. In order to understand this apparent contradiction, we repeated the starvation experiments in LB for two *E.coli* strains: the *E.coli* K-12, which has undergone many years of evolution in labs since its isolation from

the wild, and a more recent EPEC wild-type isolate. We found that starvation in LB does not lead to a disrupted state for short starvation time (typical of an overnight culture). However, starvation longer than overnight does lead to the disrupted state and ageing in the K-12 strain (Fig. S9), in agreement with our previous results[8], but not for the EPEC strain (Fig. S9). In our stress classification framework, this suggests that whereas the EPEC strain of *E.coli* is adapted to longer starvation in rich medium, the lab K-12 strain may have lost the ability to recover fast from these conditions which it does not encounter in laboratory conditions[3]. Finally, we regroup all stress conditions into one plot showing that while most conditions can be classified as leading or not to ageing (Fig. S10C), starvation of the K-12 strain in LB has an intermediate level of ageing.

Discussion

The analogy between the disrupted state of bacteria under prolonged stress and ageing in random dynamical systems that we present here (Box1) provides a new framework for the description of the response of cells to strong perturbations[45]. Clearly, random networks cannot describe regulated cellular responses that rely on specific networks. In particular, cellular networks have been recently shown to suppress frustration when compared to random networks[46]. However, once the system is driven away from its adaptive potential, frustration is not suppressed anymore and a disrupted state is reached whose dynamics are better described statistically by a random model that ignores the details of the underlying pathways. The recovery from acute stress that we observed is characterized by three main features: ageing dynamics, saturation of ageing and broad single-cell variability. All these are robust features predicted by the RCCN model. The biochemical intuition for the frustration that characterizes the disrupted state can be understood as the inability of the genetic network to regulate the compounds that allow the cell to deal with the stress, because other compounds are missing for their production or degradation. This frustration can then propagate in the network leading to a globally dysregulated state and large cell-to-cell heterogeneity.

In our experiments, the natural and gradual stresses allow the cell to reach an attractor of the gene regulation network[47] (Fig. 4J), in which bacteria are narrowly distributed around one phenotype with one characteristic lag time, as observed for the gradual starvation in

minimal medium (Fig. 4C) or gradual exposure to SHX (Fig. 4F). This growth arrested stable state has been previously shown to be different from a frozen state and to actually sustain long-term protein production at a constant rate (CASP)[48]. More generally, it is expected that regulated responses reach stability[49] (Fig. 4I). Lag time for the exit from such a gradual starvation state was shown to be mainly due to pathways associated with growth[50,51]. In contrast, the strong and abrupt perturbations (SHX /sodium azide/CAM) disrupt the network in a way that drives its dynamics away from its biological adaptation potential and closer to the generic dynamics of the large random network (Fig.4J). The dynamics of recovery of individual bacteria from the disrupted state reveal the complexity of the intracellular dynamics, resulting in a very broad lag time distribution (Fig. 4G,H). The longer the starvation time, T_w, the longer the time-scales that are reflected in the single–cell individuality leading to antibiotic persistence. At T_w longer than about a day, ageing saturates revealing, according to the RCCN model, the longest time-scale of the cellular dynamics which is surprisingly long for *E.coli*[52].The ageing dynamics features may not be related to a particular genetic pathway, but rather to the global architecture of the network. Therefore, the triggered persister cells, namely the bacteria that are protected by the extended lag time acquired following a stress, may be better described by the global dynamics of a random network rather than by a regulated response. This view is inspired by the Pash hypothesis[53], which suggested that antibiotic persistence is the result of random glitches and errors rather than of a specific genetic pathway[54]. Our results provide a new framework, with quantitative predictions, for understanding antibiotic persistence as a feature of a disrupted state, displaying the global dynamics of cellular networks far away from their comfort zone[45].

More generally, the work identifies a regime in which cellular networks under strong perturbations can be approximated by a large non-linear network that ignores most of the details of the underlying molecular interactions and for which measurements, such as specific gene expression, may reflect random dynamics[45]. Our approach suggests that similar behavior should account for different observations such as the post-antibiotic effect [55], and differences in the recovery dynamics from various starvation conditions [56]. Recent developments in single-bacteria RNAseq[57-59] may enable to further characterize the disrupted state by identifying a global state of dysregulation.

The measurement of universal ageing dynamics in a biological system, as presented in this work, can be extended to various other cellular systems under stress, such as cells under anti-cancer drugs, and should be an important tool for predictive biology[60]. The approach allows distinguishing between two very different regimes of cellular behavior that require different measurements: a regulated regime, for which the molecular information such as transcriptomics or proteomics provide insightful mechanistic information, and a disrupted regime in which cells are closer to a universal behavior similar to that of high dimensional physical systems, such as ageing and phase transitions.

Acknowledgements

We thank Brandon Seo and Johan Paulsson for the microfluidic mother-machine templates. Naama Barkai, Yoram Burak and Adi Rotem for comments on the manuscript and for illuminating discussions. This work was supported by the European Research Council (Consolidator grant no. 681819), the Israel Science Foundation (grant no.597/20) and the Minerva Foundation.

References

1 Storz, G. & Hengge, R. *Bacterial Stress Responses* (ASM, 2011).

2 Brauer, M. J. *et al.* Coordination of growth rate, cell cycle, stress response, and metabolic activity in yeast. *Mol Biol Cell* **19**, 352-367 (2008).

3 Koch, A. L. The adaptive responses of Escherichia coli to a feast and famine existence. *Adv Microb Physiol* **6**, 147-217 (1971).

4 Erickson, D. W. *et al.* A global resource allocation strategy governs growth transition kinetics of Escherichia coli. *Nature* **551**, 119-123 (2017).

5 Bigger, J. W. Treatment of staphylococcal infections with penicillin by intermittent sterilisation. *The Lancet* (1944).

6 Balaban, N. Q., Merrin, J., Chait, R., Kowalik, L. & Leibler, S. Bacterial persistence as a phenotypic switch. *Science* **305**, 1622-1625 (2004).

7 Balaban, N. Q. *et al.* Definitions and guidelines for research on antibiotic persistence. *Nat Rev Microbiol* **17**, 441-448 (2019).

8 Levin-Reisman, I. *et al.* Automated imaging with ScanLag reveals previously undetectable bacterial growth phenotypes. *Nature Methods* **7**, 737-U100 (2010).

9 Fridman, O., Goldberg, A., Ronin, I., Shoresh, N. & Balaban, N. Q. Optimization of lag time underlies antibiotic tolerance in evolved bacterial populations. *Nature* **513**, 418-+ (2014).

10 Johnson, P. J. T. & Levin, B. R. Pharmacodynamics, Population Dynamics, and the Evolution of Persistence in Staphylococcus aureus. *Plos Genetics* **9** (2013).

11 Lewis, K. Persister cells, dormancy and infectious disease. *Nature Reviews Microbiology* **5**, 48-56 (2007).

12 Brauner, A., Fridman, O., Gefen, O. & Balaban, N. Q. Distinguishing between resistance, tolerance and persistence to antibiotic treatment. *Nat Rev Microbiol* **14**, 320-330 (2016).

13 Fridman, O., Goldberg, A., Ronin, I., Shoresh, N. & Balaban, N. Q. Optimization of lag time underlies antibiotic tolerance in evolved bacterial populations. *Nature* **513**, 418-421 (2014).

14 Luidalepp, H., Joers, A., Kaldalu, N. & Tenson, T. Age of inoculum strongly influences persister frequency and can mask effects of mutations implicated in altered persistence. *J Bacteriol* **193**, 3598-3605 (2011).

15 Pin, C. & Baranyi, J. Single-cell and population lag times as a function of cell age. *Appl Environ Microbiol* **74**, 2534-2536 (2008).

16 Moreno-Gámez, S. *et al.* Wide lag time distributions break a trade-off between reproduction and survival in bacteria. *Proceedings of the National Academy of Sciences*, 202003331 (2020).

17 Lewis, K. *Persister Cells and Infectious Disease*. (Springer Nature, 2019).

18 Vulin, C., Leimer, N., Huemer, M., Ackermann, M. & Zinkernagel, A. S. Prolonged bacterial lag time results in small colony variants that represent a sub-population of persisters. *Nat Commun* **9**, 4074 (2018).

19 Potrykus, K. & Cashel, M. (p)ppGpp: still magical? *Annu Rev Microbiol* **62**, 35-51 (2008).

20 Simsek, E. & Kim, M. Power-law tail in lag time distribution underlies bacterial persistence. *Proc Natl Acad Sci U S A* **116**, 17635-17640 (2019).

21 Potvin-Trottier, L., Luro, S. & Paulsson, J. Microfluidics and single-cell microscopy to study stochastic processes in bacteria. *Current Opinion in Microbiology* **43**, 186-192 (2018).

22 Amir, A., Oreg, Y. & Imry, Y. On relaxations and aging of various glasses. *P Natl Acad Sci USA* **109**, 1850-1855 (2012).

23 Struik, L. in *Physical aging in amorphous polymers and other materials* (Elsevier, Amsterdam, 1978).

24 Hwa, T., Marinari, E., Sneppen, K. & Tang, L. H. Localization of denaturation bubbles in random DNA sequences. *Proc Natl Acad Sci U S A* **100**, 4411-4416 (2003).

25 Matan, K., Williams, R. B., Witten, T. A. & Nagel, S. R. Crumpling a thin sheet. *Physical Review Letters* **88** (2002).

26 Lahini, Y., Gottesman, O., Amir, A. & Rubinstein, S. M. Nonmonotonic Aging and Memory Retention in Disordered Mechanical Systems. *Physical Review Letters* **118** (2017).

27 Vaknin, A., Pollak, M. & Ovadyahu, Z. Memory and aging in an electron glass. *Springer Proc Phys* **87**, 995-996 (2001).

28 Cugliandolo, L. F. & Kurchan, J. Analytical Solution of the Off-Equilibrium Dynamics of a Long-Range Spin-Glass Model. *Physical Review Letters* **71**, 173-176 (1993).

29 Franz, S., Mezard, M., Parisi, G. & Peliti, L. Measuring equilibrium properties in aging systems. *Physical Review Letters* **81**, 1758-1761 (1998).

30 Bouchaud, J. P. Weak Ergodicity Breaking and Aging in Disordered-Systems. *J Phys I* **2**, 1705-1713 (1992).

31 Ackermann, M., Chao, L., Bergstrom, C. T. & Doebeli, M. On the evolutionary origin of aging. *Aging Cell* **6**, 235-244 (2007).

32 Kirkpatrick, S. & Sherrington, D. Infinite-Ranged Models of Spin-Glasses. *Phys Rev B* **17**, 4384-4403 (1978).

33 Sompolinsky, H., Crisanti, A. & Sommers, H. J. Chaos in random neural networks. *Phys Rev Lett* **61**, 259-262 (1988).

34 Kauffman, S., Peterson, C., Samuelsson, B. & Troein, C. Random Boolean network models and the yeast transcriptional network. *P Natl Acad Sci USA* **100**, 14796-14799 (2003).

35 Gabalda-Sagarra, M., Carey, L. B. & Garcia-Ojalvo, J. Recurrence-based information processing in gene regulatory networks. *Chaos* **28**, 106313 (2018).
36 Ravasz, E., Somera, A. L., Mongru, D. A., Oltvai, Z. N. & Barabasi, A. L. Hierarchical organization of modularity in metabolic networks. *Science* **297**, 1551-1555 (2002).
37 Nagar, N. *et al.* Harnessing Machine Learning To Unravel Protein Degradation in Escherichia coli. *mSystems* **6** (2021).
38 Nystrom, T. Conditional senescence in bacteria: death of the immortals. *Mol Microbiol* **48**, 17-23 (2003).
39 Schink, S. J., Biselli, E., Ammar, C. & Gerland, U. Death Rate of E. coli during Starvation Is Set by Maintenance Cost and Biomass Recycling. *Cell Syst* **9**, 64-73 e63 (2019).
40 St John, A. C. & Goldberg, A. L. Effects of reduced energy production on protein degradation, guanosine tetraphosphate, and RNA synthesis in Escherichia coli. *J Biol Chem* **253**, 2705-2711 (1978).
41 Durfee, T., Hansen, A. M., Zhi, H., Blattner, F. R. & Jin, D. J. Transcription profiling of the stringent response in Escherichia coli. *J Bacteriol* **190**, 1084-1096 (2008).
42 Nystom, T. Role of guanosine tetraphosphate in gene expression and the survival of glucose or seryl-tRNA starved cells of Escherichia coli K12. *Mol Gen Genet* **245**, 355-362 (1994).
43 Gurvich, Y., Leshkowitz, D. & Barkai, N. Dual role of starvation signaling in promoting growth and recovery. *PLoS Biol* **15**, e2002039 (2017).
44 Link, H., Fuhrer, T., Gerosa, L., Zamboni, N. & Sauer, U. Real-time metabolome profiling of the metabolic switch between starvation and growth. *Nat Methods* **12**, 1091-1097 (2015).
45 Stern, S., Dror, T., Stolovicki, E., Brenner, N. & Braun, E. Genome-wide transcriptional plasticity underlies cellular adaptation to novel challenge. *Mol Syst Biol* **3**, 106 (2007).
46 Tripathi, S., Kessler, D. A. & Levine, H. Biological Networks Regulating Cell Fate Choice Are Minimally Frustrated. *Phys Rev Lett* **125**, 088101 (2020).
47 Radzikowski, J. L., Schramke, H. & Heinemann, M. Bacterial persistence from a system-level perspective. *Curr Opin Biotechnol* **46**, 98-105 (2017).
48 Gefen, O., Fridman, O., Ronin, I. & Balaban, N. Q. Direct observation of single stationary-phase bacteria reveals a surprisingly long period of constant protein production activity. *P Natl Acad Sci USA* **111**, 556-561 (2014).
49 Guo, Y. & Amir, A. Stability of gene regulatory networks. *arXiv:2006.00018v2* (2020).
50 Sekar, K. *et al.* Synthesis and degradation of FtsZ quantitatively predict the first cell division in starved bacteria. *Mol Syst Biol* **14** (2018).
51 Madar, D. *et al.* Promoter activity dynamics in the lag phase of Escherichia coli. *Bmc Systems Biology* **7** (2013).
52 Shamir, M., Bar-On, Y., Phillips, R. & Milo, R. SnapShot: Timescales in Cell Biology. *Cell* **164**, 1302-U1235 (2016).
53 Levin, B. R., Concepcion-Acevedo, J. & Udekwu, K. I. Persistence: a copacetic and parsimonious hypothesis for the existence of non-inherited resistance to antibiotics. *Curr Opin Microbiol* **21**, 18-21 (2014).
54 Kaldalu, N. *et al.* In Vitro Studies of Persister Cells. *Microbiol Mol Biol Rev* **84** (2020).
55 Craig, W. A. The Post-Antibiotic Effect. *Clinical Microbiology Newletter* **13**, 121-128 (1991).
56 Holmquist, L. & Kjelleberg, S. Changes in Viability, Respiratory Activity and Morphology of the Marine Vibrio Sp Strain S14 during Starvation of Individual Nutrients and Subsequent Recovery. *Fems Microbiol Ecol* **12**, 215-224 (1993).

408 57 Blattman, S. B., Jiang, W., Oikonomou, P. & Tavazoie, S. Prokaryotic single-cell RNA
409 sequencing by in situ combinatorial indexing. *Nat Microbiol* **5**, 1192-1201 (2020).
410 58 Imdahl, F., Vafadarnejad, E., Homberger, C., Saliba, A. E. & Vogel, J. Single-cell RNA-
411 sequencing reports growth-condition-specific global transcriptomes of individual
412 bacteria. *Nat Microbiol* **5**, 1202-+ (2020).
413 59 Kuchina, A. *et al.* Microbial single-cell RNA sequencing by split-pool barcoding. *Science*
414 **371** (2021).
415 60 Lopatkin, A. J. & Collins, J. J. Predictive biology: modelling, understanding and harnessing
416 microbial complexity. *Nat Rev Microbiol* (2020).

417

418

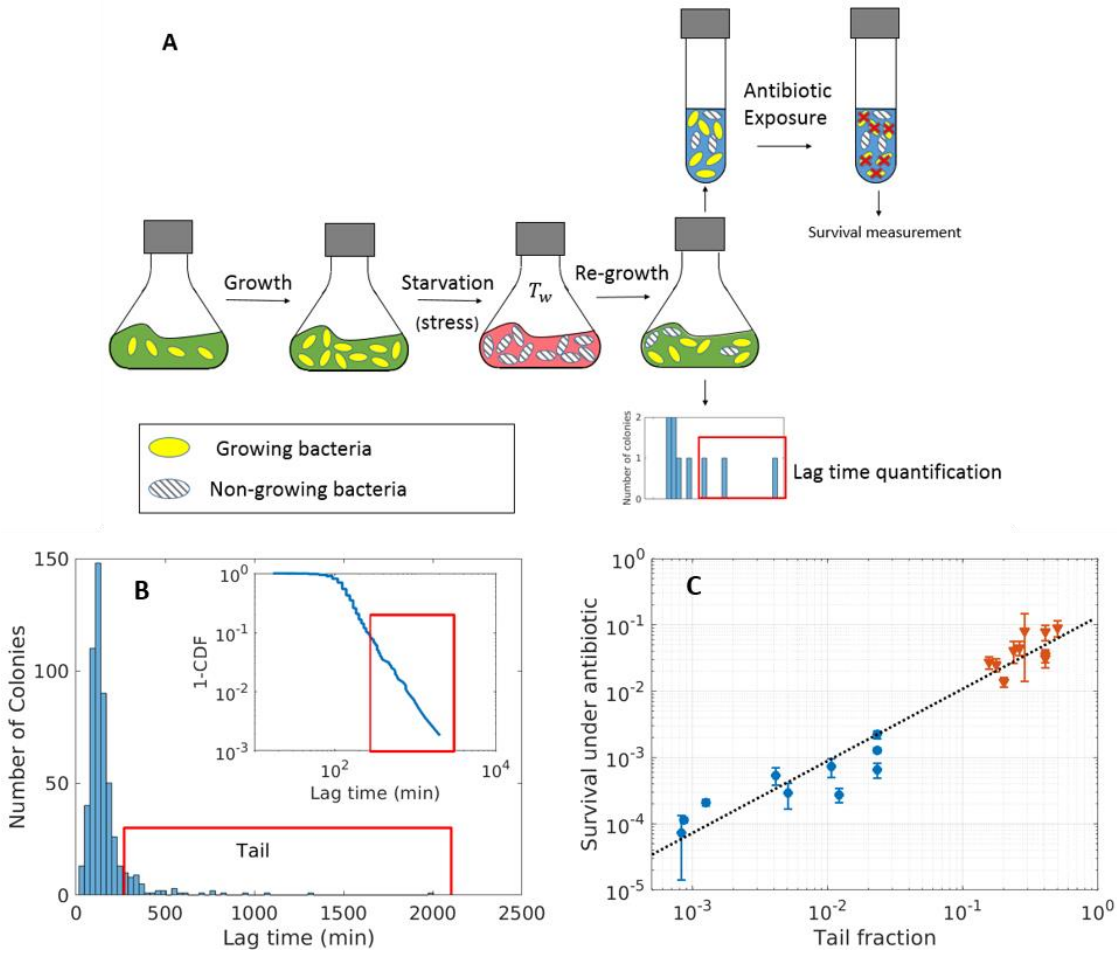

Fig. 1 The tail of the lag time distribution correlates with survival under antibiotic treatment. (A) Schematic time course: after a period of growth, the culture is starved for a duration T_w (waiting time)– where bacteria arrest their growth – and then re-exposed to nutrients. Single bacteria stochastically re-grow after a lag time. If the culture is exposed transiently to antibiotics, bacteria that re-grow are killed, whereas non-growing persisters survive. **(B)** Typical distribution of the lag time following LB starvation measured by monitoring the appearance of colonies on Petri dishes[8] (here T_w=1820 minutes). A tail of colonies appearing long after plating can be seen in the red box. Inset: same data replotted as 1- CDF (Cumulative Distribution Function), which represents the fraction of bacteria still in the lag phase, and enables better visualization of the tail of the distribution. The fraction is one at the end of starvation (all bacteria are growth arrested) and decreases to zero as bacteria exit the lag **(C)** The tail fraction of the lag time distribution (here above 4.5 h), i.e. the bacteria with a lag time longer than 4.5 h, is predictive for the survival fraction under an antibiotic treatment of the same duration. Blue circles: KLY wt- different T_w. Red triangles: KLY^{tol} high persistence derivative. Dashed line: linear regression; Pearson correlation: 0.97, $p<10^{-11}$. Spearman correlation for KLY wt and KLY^{tol}, respectively: cor=0.87, p=0.0012 and cor=0.69, p=0.026.

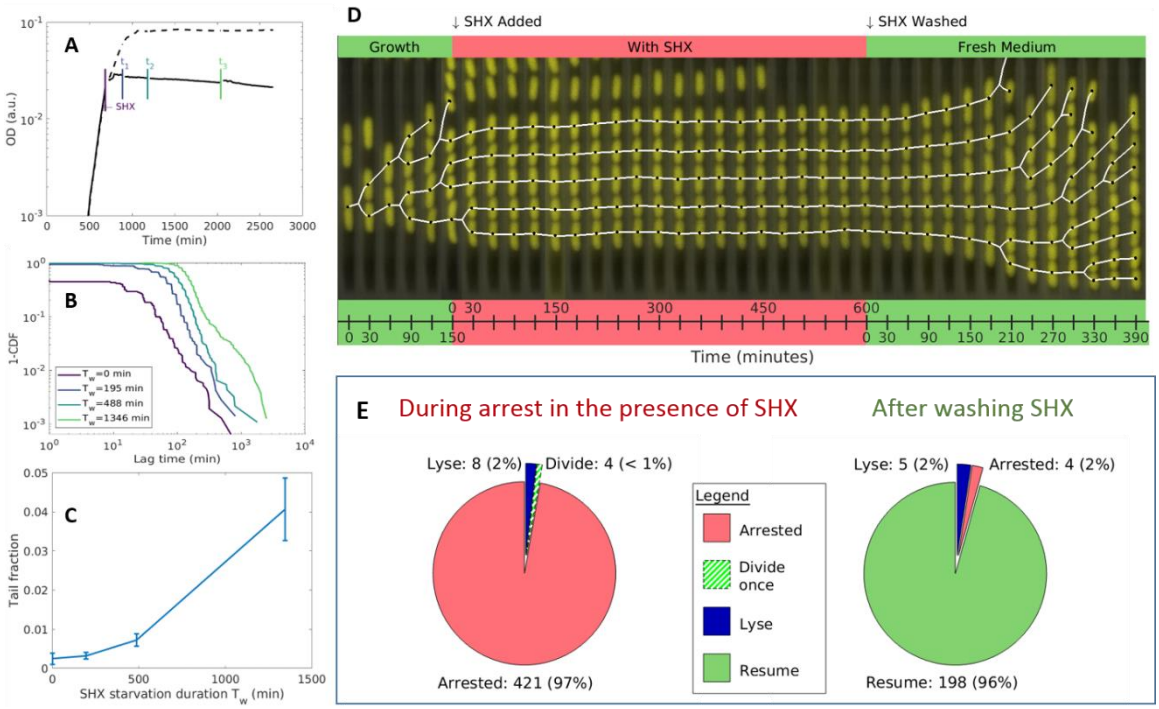

Fig. 2 Distribution of the lag time following starvation for various durations T_w of exposure to serine hydroxamate (SHX). (A) OD measurements of growth (dashed line) and arrest due to SHX exposure (solid line). **(B)** Lag time distribution for different starvation durations. Data are presented as 1-CDF (cumulative distribution function) on log scale to better visualize the tail of the distribution. **(C)** Total fraction of bacteria in the tail of the distribution shown in (B), with lag times above 9.5 hours, versus starvation duration. Error bars: std (n=3). **(D)** Kymograph of microfluidics observations of the growth arrest of single KLYR *E.coli* bacteria (yellow fluorescence) subjected to SHX and their recovery. During the initial growth phase, bacteria grow and divide in the grooves and migrate upwards. After exposure to SHX, growth stops. At T_w=600 minutes, SHX was washed and bacteria resumed growth stochastically. The black dots and white lines are guides to the eye to enable tracking the same bacterium between frames. **(E**) Quantification of growth arrest under SHX in single cells: 97% of cells arrested their growth (1%:one division only; 2% lysis); upon SHX washing, 96% resumed growth (see Supplementary Methods). All experiments were performed in at least three repeats. Strain: KLYΔmotA.

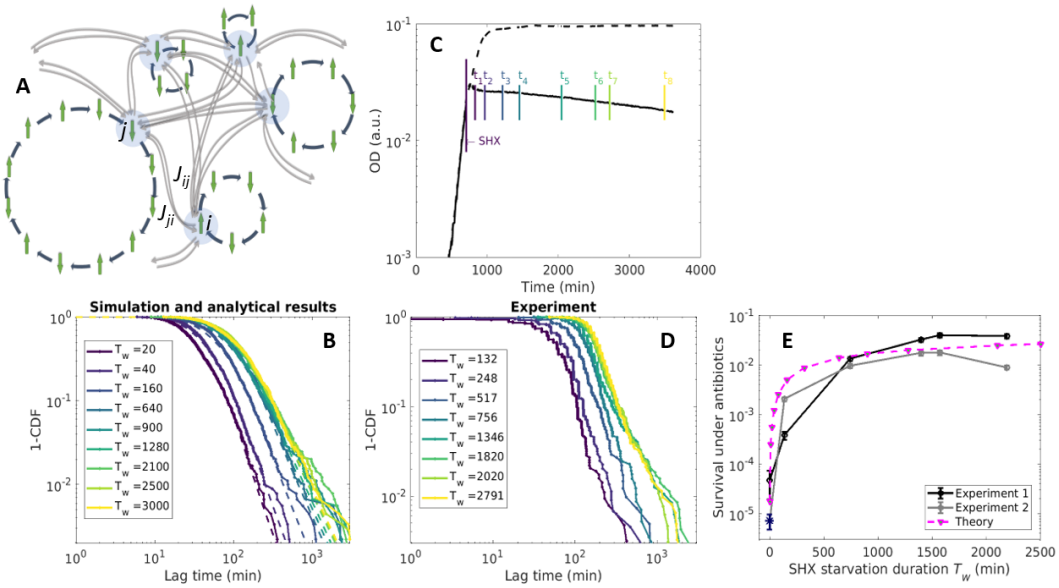

Fig.3 The Randomly Connected Cycles Network (RCCN) model reproduces the ageing dynamics observed in the experiment (A) Schematic representation of the random cycles network model: cycles of nodes are inter-connected with randomly chosen interaction coupling strengths J_{ij} (grey arrows). The dynamics of the state of each node (spin) in the network is determined by summing up on interactions with the connected nodes and external field (Eq. S5). **(B)** Prediction from the simulation for the dependence of the distribution of lag times following starvation (here plotted as 1-CDF on log-log scale). Different colours represent different T_w durations. Simulation parameters are listed in Table S2. Dashed lines are the analytical results**. (C)** OD_{630} measurements of growth and arrest due to SHX exposure. Dashed line: no SHX. **(D)** Experimental results for the distribution of lag times as measured after abrupt exposure to SHX. Note that the lag time distribution becomes independent of starvation duration for long enough starvation, as predicted by the model. Different colours represent different durations of exposure to SHX and correspond to the coloured marks of sampling times in (C)**. (E)** Measurements of the survival under 9.5 hours of ampicillin treatment during the recovery of SHX starvation versus abrupt SHX starvation duration, T_w. As predicted by the RCCN (Eq.S8) (purple dashed lines), the survival under antibiotics first increases sharply with exposure time but saturates at longer times. Different lines represent different biological replicates. Strain: KLYR.

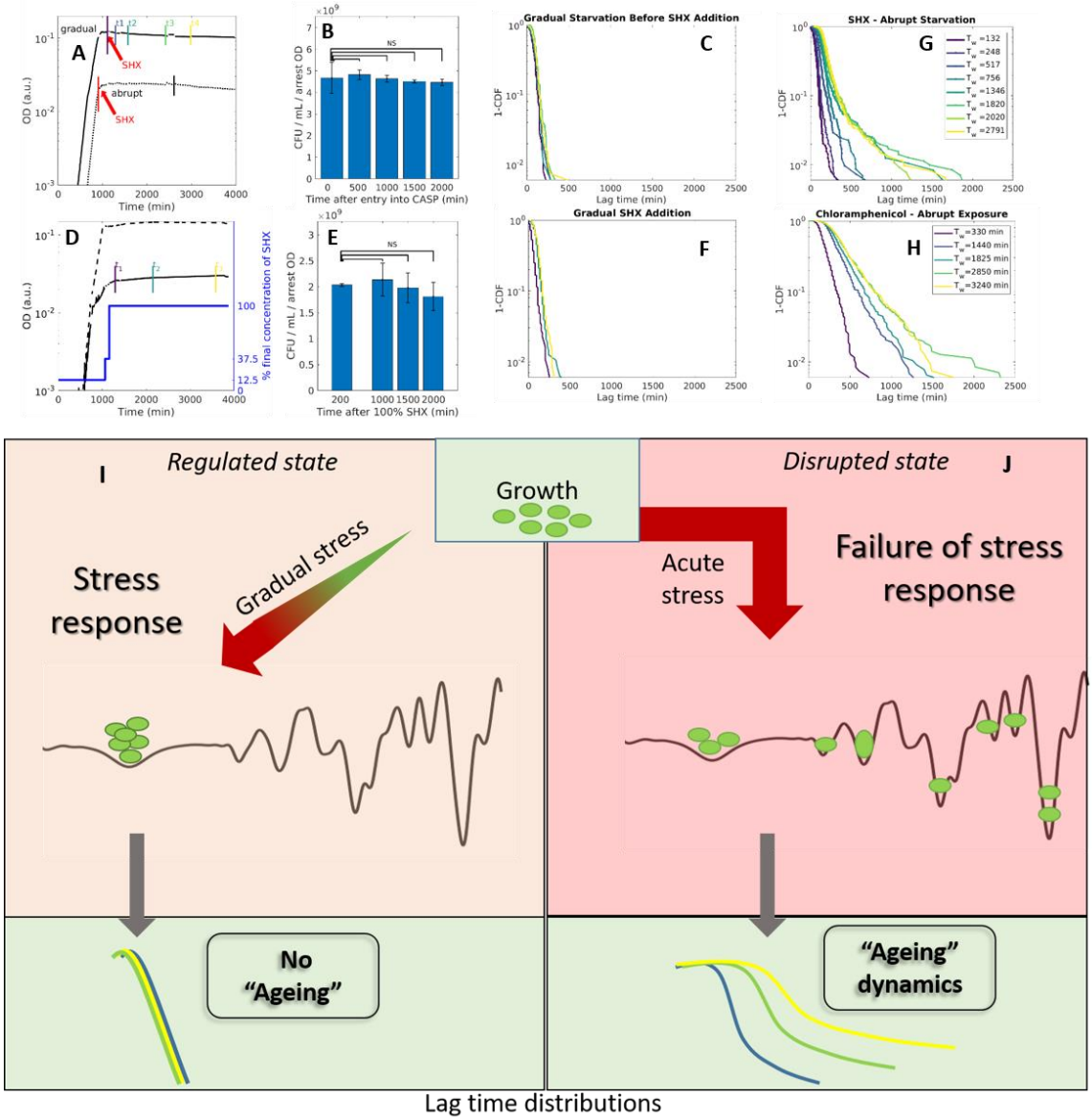

Fig.4 (A-F) No ageing under gradual starvation. (A-C) Gradual starvation by nutrient depletion. **(A)** OD measurements of bacterial cultures exposed to SHX during exponential growth (acute stress – dotted line), or exposed to SHX after gradual starvation by nutrient depletion to stationary phase (gradual stress – solid line). **(B)** Viability under gradual starvation. Significance tests over 3 biological replicates. Differences in viability are non significant (NS). **(C)** Lag time distribution after gradual starvation by nutrients depletion. The coloured curves represent different starvation durations according to colours in (A). **(D-F)** Gradual starvation by adding SHX gradually in several steps. **(D)** During exponential growth, a culture was starved gradually by adding SHX in steps, reaching growth-arrest at a low OD (solid line). Dashed line: no SHX addition. Blue line: SHX concentration. **(E)** Viability under the gradual SHX starvation. Significance tests over 3 biological replicates. Differences in viability are non significant (NS). **(F)** Lag time distribution after adding SHX gradually in steps. Strain: KLYR. **(G)** Lag time distribution after abrupt SHX starvation (Fig. 3D semi-log scale for comparison). Strain: KLYR. **(H)** Lag time distribution after abrupt

chloramphenicol exposure. Strain: MG1655. **(I-J**) **Schematic illustration of gradual starvation versus acute perturbation**. The black line shows a schematic landscape of the cell's possible states. **(I)** Gradual starvation leads single bacteria (green) to a regulated response reaching a fixed point in the cell's network characterized by a narrow distribution of lag times and no ageing. **(J)** Acute stress results in a disrupted state displaying dynamics of the cell's network similar to ageing dynamics in physical systems and broad lag time distributions that depend on starvation duration. Different colours in the lag time distributions (plotted as 1-CDF) at the bottom represent different stress exposure durations.

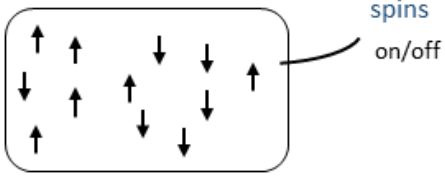 Network model	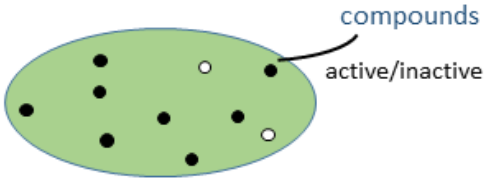 Bacterium
Interactions parameters between spins	Biochemical interactions between cellular compounds
No external force aligning the spins i.e magnetic field $H = 0$	Nutrients
No magnetization: $\bar{M} = 0$	Growth
External force applied: magnetic field switched on: $H > 0$	Acute stress
Magnetization $\bar{M} > 0$	Growth arrest
Time for M back to 0 (single realization) 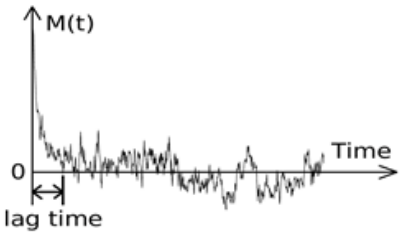	Single cell lag time to restart growth and division 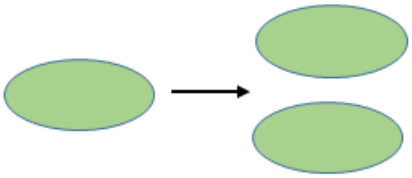

Box1: Analogy between physical ageing in a spin network and ageing of bacteria under acute stress.